

## The possibility of vessel motion data use for high resolution satellite SAR image focusing

Franc Dimc<sup>1,2</sup>, Juan Ignacio Cicuendez<sup>1,3</sup>, Harm Greidanus<sup>1</sup>, Marko Perkovic<sup>2</sup>  
Maciej Gućma<sup>4</sup>, Victor Silva<sup>1</sup>, Marek Duczkowski<sup>4</sup>

<sup>1</sup> European Commission – Joint Research Centre, Via Enrico Fermi 2749, Ispra, Italy

<sup>2</sup> University of Ljubljana, Faculty of Maritime Studies, Pot pomorščakov 4, 6320 Portorož, Slovenia  
e-mail: franc.dimc@fpp.uni-lj.si

<sup>3</sup> Earth Observation Services & Satellite-AIS Department, Hisdesat Servicios Estratégicos, S.A.  
Madrid 28046, Spain

<sup>4</sup> Maritime University of Szczecin, ul. Wały Chrobrego 1–2, 70-500 Szczecin, Poland

**Key words:** high resolution SAR imaging, integrated motion sensors

### Abstract

Maritime surveillance from space is useful for many applications, such as fisheries control, maritime border control and maritime security. A new generation of satellite-borne Synthetic Aperture Radars is able to provide resolutions of down to 1 meter. In the case of maritime targets, however, their motions lead to blurring in the SAR images, so these high resolutions cannot be attained. Scientific research into how to surmount the existing limits on the use of high-resolution images for maritime surveillance would be of great utility. In this context, high resolution SAR data were collected from ships that have been fitted with motion sensors in order to understand vessel motion impact on detection and recognition capability.

### Introduction

Maritime surveillance is currently much in demand for fisheries control, border control, pollution control, anti-terrorism and related maritime security and safety fields. The seas and oceans being so vast, maritime surveillance assets are in relation scarce and expensive – there is always a lack of awareness, especially in areas away from the coast and for smaller targets. Therefore, people look for earth observation satellites to help collect information. The most relevant type of earth observation satellite for maritime surveillance is Synthetic Aperture Radar (SAR), because it is independent of clouds or daylight, and because it can have a high resolution even from a far distance. Consequently, many satellite SARs are now available or planned – ENVISAT-ASAR, Sentinel-1, Radarsat-1, -2 and -3, TerraSAR-X, CosmoSky-med, Paz and more. The newer of these have ever higher resolutions – TerraSAR-X and Radarsat-2 – e.g., down to 1–2 m. These high resolutions enable the detection of small targets, and the classification of larger ones.

However, with maritime targets there is a problem. The SAR obtains its high resolution based on the integration of the radar signal over time – it can take many seconds of observing a target from different angles by the moving radar in order to collect the necessary data. For stationary targets, this is no problem. Ships, however, in motion are problematic – besides their linear motion as they sail, they also rotate (pitch, roll and yaw) as the ocean waves move them. These motions during the SAR integration time, especially the rotations, cause distortions, resulting in blurring (de-focussing). The greater the ship's motions and the longer the integration time (needed for higher resolutions), the more the blurring. This de-focusing obviously precludes the attainment of the desired high resolution. Indeed, it is a well-known phenomenon that small ships often appear as blurs instead of dots, even in medium resolution SAR images. Due to this effect, the new high-resolution SARs essentially don't work on moving ships.

If the motions of the target are known, then in some cases the SAR processing can be adapted in order to yield well-focussed images after all.

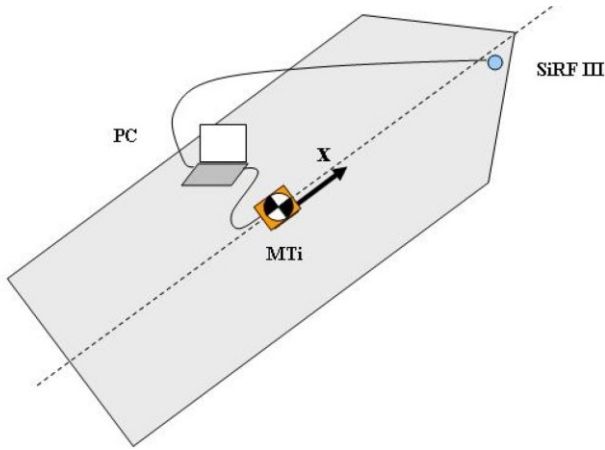


Fig. 1. A typical placement scheme for the sensors and equipment aboard

Alternatively, the ISAR (Inverse SAR) technique uses the target rotation, estimated from the data itself, to image the target. With this in mind, the present study was provided the task of collecting SAR data from small ships while at the same time measuring their detailed 3D motions, the aim being to attempt an improved focussing of the target SAR images, testing whether the recorded motion data were able to produce well-focussed images.

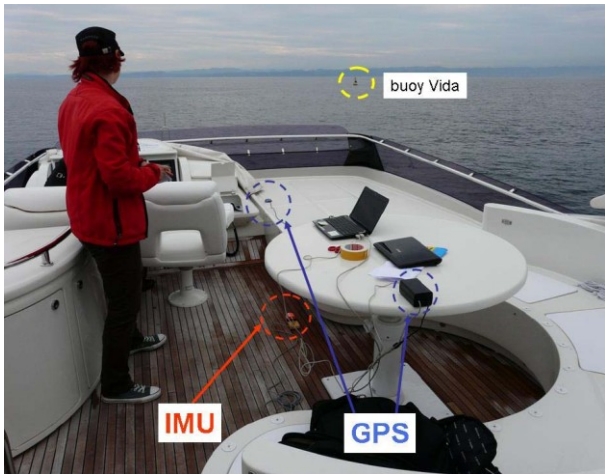


Fig. 2. A vessel Dominator 68 approaching the oceanographic buoy, before acquisition No. 7

## Data collection overview

Between May 17 and June 6, 2010, a total of 7 satellite SAR images were acquired over the northern Adriatic, close to the oceanographic buoy "Vida" operated by the Slovenian National Institute of Biology. Acquisition times were around 05 and 17 UTC, related to the satellite orbits. At the times of the satellite overpasses, several small and medium-sized boats were deployed in the sea area that was imaged. The boats carried instrumentation to measure their positions and motions. The SAR image acquisition only takes a few seconds. Within

that period, the satellite-borne SAR that travels at about 700 km altitude at an orbital speed of 7.5 km/s illuminates the target with several thousand radar pulses per second, and records the received echoes. Only the detailed motion of the ships within those few seconds, then, is of relevance to compare with the SAR data. The relative cross-range and range motion of the satellite mass centre regarding the vessel's mass centre were captured by the geo-referenced sensors while the satellite velocity  $V$  (see Eq. 1) was reported by the satellite operator.

## SAR imaging model for moving targets

In order to isolate the factors which are relevant for defocusing of moving vessels in SAR imagery, the following model for a moving punctual target is proposed in [1], where a model of the side-looking SAR-vessel range  $R$  variation with time that includes  $r$  indexed range,  $c$  indexed cross-range relative motions and the SAR velocity  $V$ :

$$R^2(t) = \left[ Vt - v_c t - \frac{1}{2} a_c t^2 \right] + \left[ R_0 - v_r t - \frac{1}{2} a_r t^2 \right] \quad (1)$$

Doing a series expansion of the above equation where only quadratic terms are retained and normalised, the following expression can be derived:

$$R(t) \cong R_0 - \varepsilon_{\dot{r}} \cdot x + [(1 - \varepsilon_c)^2 - \varepsilon_{\ddot{r}}] \cdot \frac{x^2}{2R_0}, x \in V \cdot T \quad (2)$$

Where  $T$  is the integration time and with the following normalised coefficients:

$$\varepsilon_{\dot{r}} = \frac{v_r}{V} \quad (\text{Doppler or radial velocity})$$

$$\varepsilon_{\ddot{r}} = \frac{a_r \cdot R_0}{V^2} \quad (\text{Radial acceleration})$$

$$\varepsilon_c = \frac{v_c}{V} \quad (\text{Cross-range velocity})$$

The returned signal that depends on the cross-range (azimuth) direction can be represented by:

$$m(x) = a(x) \exp(-j2k \cdot R(t)) \quad (3)$$

Being  $k = 2\pi/\lambda$  the wave number and  $a(x)$  is the azimuth antenna weighing. Finally, taking into account that the cross-range speed affects the antenna azimuth weighing and equation (2), the received signal from a moving target for the cross-range coordinate results in:

$$m(x) \cong a[(1 - \varepsilon_c) \cdot x] \exp(-j2k\varepsilon_{\dot{r}} \cdot x) \cdot \left\{ \exp(jk \frac{x^2}{R_0} \cdot [(1 - \varepsilon_c)^2 - \varepsilon_{\ddot{r}}]) \right\} \quad (4)$$

As opposed to a static target (all speeds and acceleration are zero), the above formula presents:

- A scaling factor affecting the azimuth antenna pattern.
- A ramp (associated to an azimuth displacement of the target due to the radial velocity factor  $\varepsilon_r$ ).
- A defocusing effect related to  $\varepsilon_c$  and  $\varepsilon_r$ .

The above equation (4) represents a linear frequency modulated (LFM) chirp that has a slope that differs from the static point target case in the factor  $[(1 - \varepsilon_c)^2 - \varepsilon_r]$ .

### Onboard data collection

The experiments were scheduled due to the availability of high performance satellite SAR imaging and its time optimization for the selected area. The dynamics and in some cases wind data were collected onboard and were also compared with the data from the oceanographic buoy. The six degrees of freedom MTi sensor has an internal low power signal processor which enables drift-free 3D orientation together with calibrated 3D acceleration, 3D rate of turn and the 3D earth-magnetic field data.

The MTi inertial sensors equipment used act as an attitude and heading reference system of the involved vessels. Inertial data were affected by the lever arm since the sensors were placed only as close as possible to the vessel mass centre. The raw inertial navigation data from the MTi with high a data rate (400 Hz) were stored in a laptop for post processing. With tight MTi fixing on the absorbing material the high frequency vessel engine vibrations were mainly rejected. Residual higher harmonics were treated with a Kalman filter (Fig. 3) according to the observed sea wave oscillations also

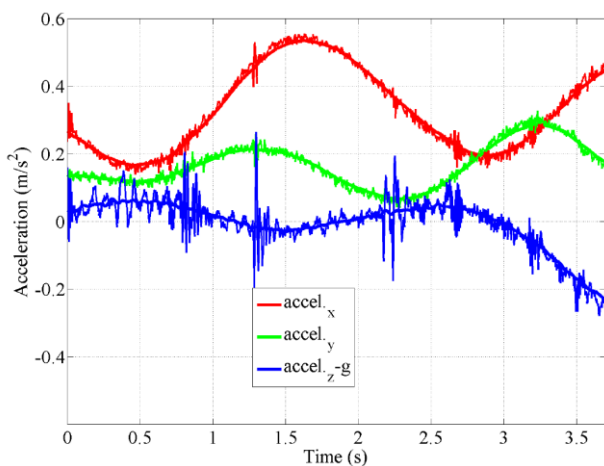


Fig. 3. An example of measured and Kalman filtered vessel accelerations during the acquisition time No. 4

obtained from the oceanographic buoy. For the purpose of positioning, the GPS receivers (SiRFIII, HaiCom) were attached on the deck of the selected vessels. A code was developed to synchronize the captured data samples.

According to the results acquired, the equipment used (MTi sensor, Xsens) yielded the data values within the required bounds and the ‘least-squares’ navigation systems integration [2] is established. Involving Matlab, the raw and processed data are sorted and kept ready. The ECEF is chosen as the most suitable coordinate frame for the future satellite and terrestrial sensors data fusion.

Since the experiments were determined for several ships simultaneously, crews were instructed to acquaint them not only with the regular procedure of capturing the ground truth data but also with the equipment limitations. In order to get more reliable trigger pulse lengths for the MTi a divided 1 pulse per second clock output of the spare GPS receiver (Antaris, ublox) was applied.

### Satellite SAR data collection

The acquired images comprised three TerraSAR-X “High resolution Spotlight”, three Radarsat-2 “Spotlight” and one Radarsat-2 “UltraFine”. Their main spatial features can be found in the table 1.

Polarisations were HH and HV, which are characterised by getting a generally high ship-sea contrast. The products were delivered in SLC (Single Look Complex) format, which means that many of the instrument corrections have been applied, while most of the original information needed to perform re-focussing is still preserved. The construction of a Synthetic Antenna during the satellite flight allows the SAR systems to achieve high resolution in the azimuth direction that otherwise would be impossible due to the limitation of the physical size of the antenna. In the field of high resolution SAR imagery there are two modes of special importance: Stripmap and Spotlight; both were used in the experiment.

Table 1. SAR imaging modes

Sensor	Mode	Scene size (km × km)	Range resolution (m)	Azimuth resolution (m)
Radarsat-2	Ultrafine	20 (azimuth) × 20	1.6	2.8
	Spotlight	8 (azimuth) × 18	1.6	0.8
Terrasar-X	High-Res Spotlight	5 (azimuth) × 10	1	1

## Satellite Image Processing

The key in the SAR processing lies in the use of an emitted LFM pulse and the SAR geometry of observation. After being reflected off the target's surface, the pulse returns to the antenna and is correlated with an original copy of the emitted pulse (corresponding to a static target) by what is called the match filtering technique (pulse compression) [3]. While the LFM pulse in range is generated by the hardware of the radar itself, in azimuth the received signal also presents the same linear modulation (Eq. 4); but in this case due to the acquisition geometry (Doppler shift of the target signal), the same type of filter could also be applied in the azimuth axis to obtain the final image (in this case, filter parameters are the satellite speed and the distance).

The range pulse length is of the order of microseconds, so can be viewed as instantaneous in respect to the ship and sea motions. The longer time in which the target is illuminated by the radar beam in order to achieve high azimuth resolution, however, makes the system prone to be affected by phase errors due to unexpected variations in the radar to target distance  $R$  (see Eq. 1).

The convolution of the Eq. 4 with the static target match filter applied in common SAR processing yields:

$$m(t) = a_c \cdot \exp(-j\omega_0 \cdot t + \phi_e(t)) \quad (5)$$

Therefore, the moving target is affected by the error phase  $\phi_e(t)$  that is directly related to the  $\varepsilon_r$  and  $\varepsilon_f$  which represent movement components of  $R$  and causes blurring of the target which is being imaged. At sea the main reason for variations in  $R$  is due to vessel movement caused by sea waves.

One of the main objectives of the experiment was the testing of different SAR processing methodologies (called autofocus algorithm in the SAR context) that correct those unknown errors ( $\phi_e(t)$ ), therefore, correcting blurring and increasing image contrast of vessel targets. Several methodologies were tested, and the one that proved to achieve the best results was the Phase Gradient Autofocus (PGA). In this case, the autofocus methodology was adapted in order to be applied locally on the small image areas containing the ships. PGA uses the properties of the Fourier transform in order to estimate the derivative of the azimuth phase error function. By integrating this function the error can

be extracted. In order to ensure robustness a certain degree of signal to noise ratio (SNR) is needed; therefore, the algorithm uses the strongest scatterers in a number of range cells and adds them together.

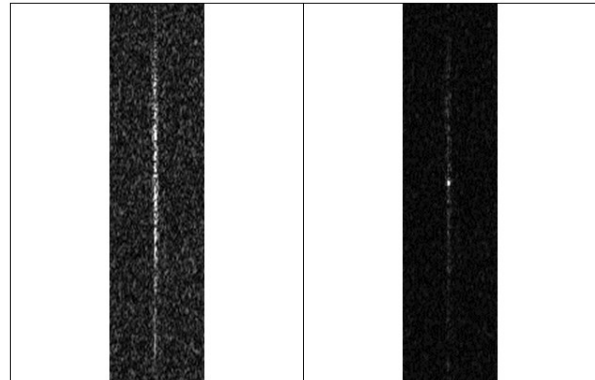


Fig. 4. The 10 m vessel Solaria in Radarsat-2 spotlight. Left – blurred by the movement, right – after application of PGA

## Conclusions

Concerning the auto-focusing of individual ships, based on the SLC data yet without using any measured motion data, this was successful in many cases (e.g. Fig. 4), but less successful in others (leading to only marginally improved de-blurring). The successful cases demonstrate that with dedicated processing, it is possible to extract significantly more information about the detected target from the SAR image than what is seen in the standard-processed images. The unsuccessful cases are attributed to low signal-to-noise, complex (fading) scattering from the ship, or a dominance in the backscatter involving the water surrounding the ship as compared to backscatter from the ship only. Further studies involving the combination of the measured motions with the SAR signature are still underway and the observed vibrations by the sensors (e.g. Fig. 3) would be treated [4].

## References

1. RANEY R.K.: Synthetic aperture imaging radar and moving targets. IEEE Trans. Aerosp. Electron. Syst., 1971, AES-7, 499–505.
2. GROVES P.D.: Principles of GNSS, Inertial, and Multisensor Integrated Navigation Systems. Artech House, Boston–London 2007, 420.
3. CURLANDER J.C, McDONOUGH R.N.: Synthetic aperture radar: systems and signal processing. Wiley series in remote sensing, Wiley, New York 1991.
4. SUBOTIC N.S., THELEN B.J., CARRARA D.A.: Cyclostationary signal models for the detection and characterization of vibrating objects in SAR data. Conference on Signals, Systems & Computers, 1998, 2, 1304–1308.